HOW DOES NIOBIUM IMPROVE THE OXIDATION RESISTANCE OF COMMERCIALLY PURE TITANIUM?

DEVELOPMENTS IN TITANIUM RESEARCH AND APPLICATIONS IN GERMANY

C. Siemers[1], J. Kiese[2]

[1]Technische Universität Braunschweig, Institut für Werkstoffe, Langer Kamp 8, 38106 Braunschweig, Germany
[2]VDM Metals GmbH, Westendstrasse 15, 45143 Essen, Germany

Keywords: Titanium, CP Titanium, Titanium Alloys, Ti 6Al 4V, Ti 6Al 2Sn 4Zr 6Mo, Ti 10V 2Fe 3Al, Ti 15Mo, Titanium Aluminides, γ-TiAl, Rapid Prototyping, Powder Metallurgy, Thermohydrogen Treatment

Abstract

In this plenary paper, advances in research, development and applications of commercially pure titanium, titanium alloys and titanium aluminides, which have occurred since the Ti-2011 World Conference on Titanium held in Beijing, China, are discussed. Information is given on important achievements in the German titanium industry, governmental and non-governmental research organisations and universities from the last four years.

Research focused on the development of new alloys mainly for aerospace and medical engineering. To reduce the production costs of conventional titanium alloys, advanced processes like electron beam melting or investment casting have been introduced into industrial production and rapid manufacturing as well as multi-material design have been intensively investigated. Forgings of intermetallic γ-TiAl based alloys allow its application in low pressure turbine blades in the geared turbofan. Finally, the feasibility of titanium scrap recycling has been studied.

Introduction

In the last few years the world's titanium industry has grown mainly driven by the aerospace industry. Consequently, since the last Titanium World Conference 2011 in Beijing, the German titanium community has continued to increase its output in leading edge titanium research and technology (see Figure 1). Multidisciplinary research activities have been carried out by the German titanium industry, research organisations and higher education establishments. Collaborations are, in addition, more and more expanded to European and international institutions.

Figure 1. Electron beam cold hearth remelting facility (EBCHR) of VDM Metals GmbH installed in their production plant in Essen, Germany.

In Germany, titanium alloy production starts from titanium sponge which is imported mainly from America and Asia. VDM Metals GmbH is Germany's largest titanium producer. Besides several four metric tons vacuum arc remelting furnaces (VAR), a new electron beam cold hearth remelting facility (EBCHR) equipped with six powerful electron guns has been installed successfully (see Figure 1). Its capacity is approx. 5000 metric tons per year. During operation, titanium sponge, master alloys, individual alloying elements as well as titanium scrap, compacts of chips and micro components or a mixture of sponge and scrap can be fed into the melt section. Typical products are blocks of rectangular shape with a length of more than five meters as well as round bars with a weight of more than twelve tons which are afterwards thermo-mechanically processed. Mainly CP Titanium as well as alloys like Ti 6Al 4V are produced.

In addition, the GfE Metalle and Materialien GmbH is producing master alloys, advanced titanium alloys and titanium aluminides in smaller quantities. Here, several VAR furnaces with capacitates up to 500 kilograms, VAR skull melters and vacuum induction melting furnaces (VIM) up to 2 metric tons are operated.

Semi-finished products, forgings, investment castings as well as machined components of several alloys for the different industrial applications are manufactured by e.g. the Otto Fuchs KG, the Alcoa AG (the former TITAL Company), MTU Aero Engines AG or Rolls Royce Germany.

Fundamental as well as applied research activities are carried out at German research organisations like the Fraunhofer IFAM, the Helmholtz Center Geesthacht or the German Aerospace Center (DLR) and several German and European universities.

New alloys have been developed, produced and introduced into industrial applications. Production costs of conventional titanium parts were reduced by the introduction of advanced processes like electron beam melting or investment casting. Forgings of intermetallic γ-TiAl based alloys allow its application in low pressure turbine blades in the geared turbofan. Rapid manufacturing, powder metallurgy and multi-material design have been investigated.

In the following sections, major developments and selected (joint) research projects of the last four years are highlighted and briefly described. Further information can be obtained from the individual conference papers and the related conference presentations.

Alloy Development

Oxidation-resistant and Microstructural-stabilized Alloy

The application of conventional titanium alloys is limited to 550°C due to their poor oxidation resistance. In addition, severe grain growth is observed in single-phase titanium alloys in long-term runs at elevated temperature leading to a degradation of their mechanical properties. In exhaust applications in automotive or aerospace engineering, products are often manufactured by cold-deformation like deep-drawing or rolling which is normally difficult in oxidation-resistant titanium alloys due to the presence of titanium-silicides. Therefore, at VDM Metals GmbH together with the TU Braunschweig, new titanium alloys based on CP-Titanium Grade 1S (soft grade) were developed showing improved oxidation resistance due to a concerted addition of silicon, iron and niobium. Microstructure stability is achieved by the precipitation of nano-size hafnium-silicides (Hf_5Si_3) mainly on the grain boundaries. Heat treatments at 800°C for 100 hours did not lead to grain growth. Finally, good cold-deformation properties are ensured due to low amounts of interstitials, e.g. oxygen. A German patent application has been submitted. The industrial production route was developed; a first five ton ingot has been produced and deformed by hot rolling (see Figure 2) so that the new class of Ti-Si-Fe-Nb-Hf alloys is now ready for application in exhaust systems of planes or cars at minimum 800°C.

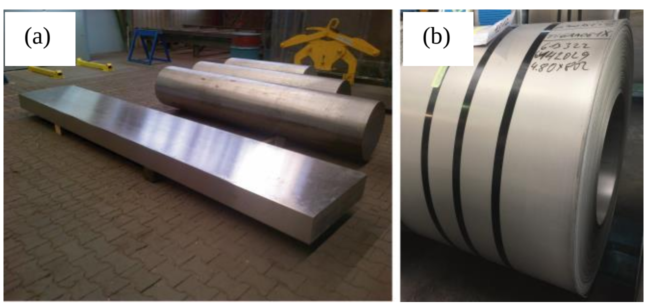

Figure 2. Industrial production of the new oxidation-resistant and microstructural-stabilized Ti-Si-Fe-Nb-Hf alloy at VDM Metals GmbH. (a) Forged slab of approx. 3.5 tons, (b) hot-rolled strip.

Aluminium- and Vanadium-free Alloys for Medical Applications

Beyond all metals, titanium alloys are the most suitable materials for osteosynthesis applications due to their excellent corrosion resistance and biocompatibility. This can be explained by the thin oxide layer being present on the surface of titanium parts. Alloys used in medical engineering are CP-Titanium, Ti 6Al 4V or Ti 6Al 7Nb. During surgery or due to inflammations the oxide layer might be damaged so that metal ions can infiltrate the blood circuit. Therefore, the use of aluminium in alloys applied in the human body is intensively discussed as it is suspected to cause Alzheimer's disease and breast cancer. Vanadium is known to be cytotoxic [1]. The Osteosynthese-Institut, Litos/ Company and their academic partners have developed new titanium alloys based on CP-Titanium Grade 4 (see Figure 3). These alloys (called CP-Titanium Grade 4^+) contain only elements which are already present in the human body, like oxygen or carbon, or that are known to be non-toxic, e.g. gold, iron or niobium. A related alloy composition is Ti 0.4O 0.5Fe 0.08C 0.1Au with the following mechanical properties: YTS: 720 MPa, UTS: 805 MPa at an elongation at rupture of 19%. Implants like bone plates have been manufactured and show excellent performance (see Figure 3). A German patent application has been submitted and the medical certification procedure was started [2].

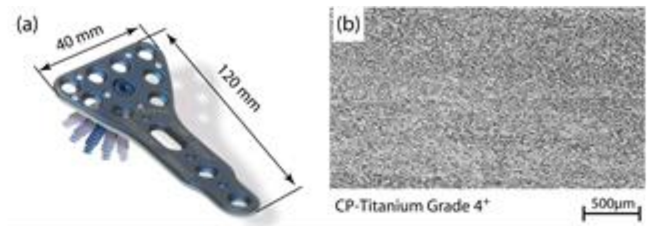

Figure 3. (a) Bone plate of Litos Company, (b) microstructure of the new class of titanium alloys (CP-Titanium Grade 4^+) after rolling and recrystallisation.

Advanced Processes and Products

Forgings of Intermetallic γ-TiAl Based Alloys

The alloy class γ-TiAl is in use for aero engines. The first application of a forged γ-TiAl alloy in an aero engine has recently been introduced by Pratt & Whitney for the Geared Turbofan (GTF_{TM}). MTU Aero Engines AG is responsible for the design and manufacturing of the low pressure turbine (LPT) and has introduced a forged γ-TiAl blade in the last row of the LPT following a joint technology program with Pratt & Whitney (see Figure 4).

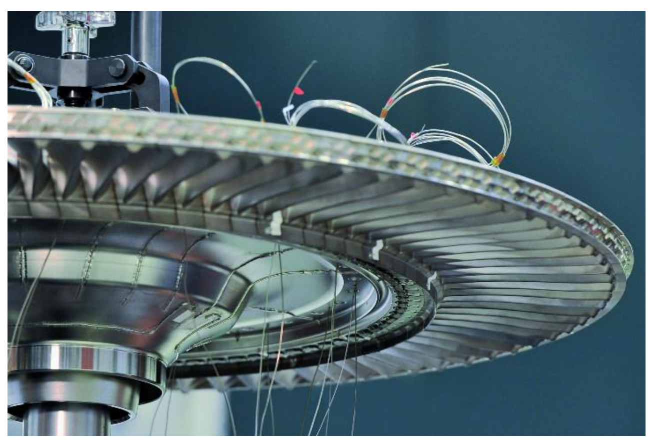

Figure 4. TNM low pressure turbine blades of the Geared Turbofan (GTF_{TM}).

The GTF uses an advanced reduction gearbox that decouples the engine's fan and LPT allowing both components to run at their respective optimum speed: low speed for the fan, high speed for the LPT. This results in significant improvements in fuel burn, pollutant and noise emissions, and operating costs.

Weight savings realized for turbine blades translate into additional weight savings throughout the turbine. Due to the high rotational speed of the LPT blades in the GTF, weight savings are more pronounced than in conventional engines. The intermetallic titanium aluminide alloy TNM (its main components are titanium, aluminum, niobium and molybdenum) has been introduced into the PW1000G-JM engine, which has been certified in December 2014.

TNM is a 3rd-generation, β-phase-containing alloy, which was developed in collaboration with the Montan University of Leoben, Austria. This alloy combines good processing capability with balanced mechanical properties. Different microstructures obtained by variation in heat treatment allow tailoring the mechanical properties according to the requirements of the intended application [3-5].

3D Screen Printing and Titanium Powder Metallurgy

Powder metallurgy, particularly Additive Manufacturing (AM) methods are more and more becoming suitable technologies for the fabrication of complex shaped titanium parts. Despite high prices for titanium powders such methods can be cost effective due to material savings and no or less machining. Most common technologies are based on selective laser or electron beam melting in which parts are generated layer by layer out of a powder bed. Unfortunately, the production of small intricate structures is still restricted to prototyping and small series productions. Unlike these beam methods in which all parts are worked out separately on a base plate, another additive manufacturing method, the so-called three dimensional screen printing, allows the simultaneous printing of several parts.

3D screen printing of titanium is developed at Fraunhofer IFAM in Dresden, Germany, and it is based on conventional two dimensional screen printing which is used in photovoltaics. A printing paste based on metal powder, binder and additives is printed layer by layer through a structured design mask (see Figure 5). By changing the screen during the printing process, overhangs or cooling channels can be integrated without the need for supporting structures and cleaning of excess powder in the end. Finally, the structures are debinded and sintered to nearly dense parts similar to metal injection moulding (MIM). Achievable minimum feature sizes for titanium are 100 µm (see Figure 6) whereas for structures less than 5 mm in diameter several 100.000 parts can be printed per year.

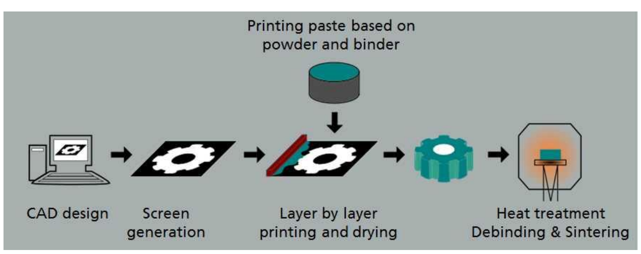

Figure 5. Scheme of the 3D screen printing technique.

One of the greatest challenges in powder metallurgy of titanium and titanium alloys is its high affinity to oxygen and, therefore, the control of material properties. Interstitial oxygen strongly decreases the ductility [6]. Thus, the oxygen levels should be kept below 0.3 wt-% (ASTM B817). The production of small intricate parts requires very small powder sizes with higher specific surface areas and higher oxygen contents. Especially, for binder based methods like 3D screen printing or metal injection moulding (MIM) an additional oxygen ingress due to organic binders is hardly preventable [7].

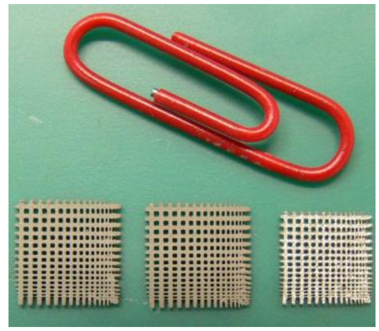

Figure 6. Demonstration objects produced by 3D screen printing.

Additionally, for small parts, free sintering promotes grain growth. Considering the above mentioned 100 µm walls in the 3D screen printed structures only a few grains are expected to develop over the wall thickness leading to lower fatigue performance [8]. To control the microstructure mostly alloying with boron or metal oxides is advisable [9, 10]. Besides, investigations to oxygen scavenging particles based on rare earth elements are discussed [11]. The disadvantage of all is the change of standardized compositions. Hence, alloying with grain pinning elements requires new qualification procedures and certification of the materials used [12].

Fraunhofer IFAM in Dresden is dealing with these problems. Efforts have been made to reduce the oxygen content of 3D screen printed and sintered Ti 6Al 4V parts using a pre-alloyed, gas–atomized powder with medium particle sizes of about 12 µm. Thus, 99% dense parts with less than 0.2 wt-% in oxygen and a homogeneous fine grained microstructure by using thermohydrogen processing could be achieved [6].

Thermo-mechanical Treatments and Manufacturing

Thermohydrogen Treatment (THT)

Increasing demands for better performance of components and structures necessitate innovative routes of thermomechanical processing. In the present study at the Universität Siegen, hydrogen is used as a temporary alloying element within the heat treatment, referred to as Thermohydrogen Treatment (THT). It facilitates the improvement of mechanical properties of the solute-rich, metastable β-titanium alloy Ti 3Al 8V 6Cr 4Mo 4Zr (β-C) by means of microstructure modification, because β-titanium alloys feature excellent characteristics concerning kinetics and thermodynamics of hydrogen sorption. This alloy class can be heat-treated to a broad range of strength to ductility ratios, whereby duplex aging consisting of the low and high temperature aging is the best conventional heat treatment method to establish a more homogeneous distribution of strengthening α-precipitates [13].

According to Figure 7a, the THT strategy hydride-induced alteration of dislocation arrangement (HADA) contains five treatment steps: recrystallization, diffusion controlled hydrogenation, hydride formation based on the hydrogen-induced redistribution of alloying elements, dehydrogenation and aging [14]. The volume effects associated with hydride formation lead to local matrix deformation accompanied by accumulation and pile-up of dislocations. The hydride-induced change of the dislocation arrangement is still present after hydride dissolution and complete hydrogen release during dehydrogenation. Hydride-induced β-crystal lattice distortion intensifies the precipitation of refined homogeneously distributed α-particles without any formation of grain boundary α-phase (α_{GB}) (see Figure 7b). This microstructure modification results in the enhancement of the fatigue limit of about 11% compared to the duplex-aging cycle. In contrast, the optimized time-consuming duplex aging leads to the formation of micro-precipitate-free zones (PFZ) accompanied by a nucleation and a growth process of the acicular a phase (see Figure 7c).

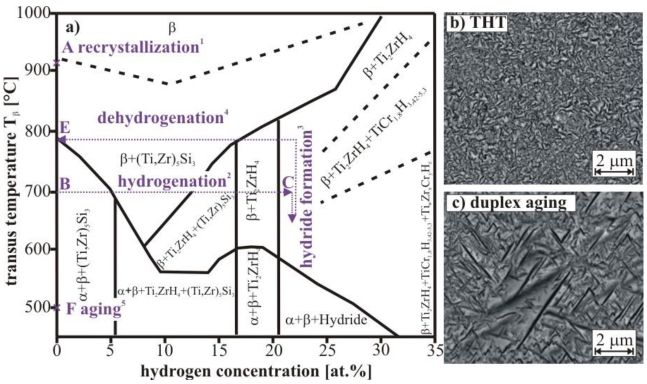

Figure 7: (a) Tβ as function of the hydrogen content; HADA-THT strategy of β-C is marked schematically by ABCDEF; (b) microstructure finally obtained after 5-step HADA-THT; (c) reference microstructure after duplex-aging cycle.

In order to broaden the applicability range of Ti 10V 2Fe 3Al, innovative routes of thermomechanical processing are necessary. The object of the present study is the hydrogen-induced microstructure modification by means of THT in order to improve the mechanical properties under monotonic and cyclic loading conditions. The formation of hydrogen-induced phases precipitating preferentially at grain and phase boundaries as a consequence of hydrogen supersaturation and eutectoid decomposition play an essential role in the successful implementation of THT. The THT process hydrogen-induced recrystallization of β phase (HIRB) shown schematically in Figure 8a comprises five treatment steps: solution treatment, hydrogenation accompanied by the precipitation of the hydrogen-induced phase (see Figure 8b), recrystallization (see Figure 8c), dehydrogenation and aging [15]. The diffusion-controlled hydride formation (TiFeH and $TiFeH_2$) accompanied by a volume expansion up to 25% [16] causes crystal lattice distortion around hydrides associated with an increased dislocation density. The recrystallization of the β phase accompanied by the complete hydride decomposition can be related to the high dislocation density comparable to the condition after cold working. In comparison to the technical heat treatment, the HIRB-THT process results in the minimized volume fraction of α_{GB} phase and completely dissolved globular primary α-phase (α_P) accompanied by a suppression of β grain coarsening. The increased age hardening of the fine-grained β matrix and the reduced volume fraction of α_{GB} phase may improve the fatigue strength in the HIRB-THT condition.

Figure 9 shows the results of fatigue tests performed under symmetrical tension-compression conditions according to the modified staircase method. In contrast to our expectations, the improvement of fatigue life is not strongly pronounced by the hydride-induced microstructure modification that can be related to the observed preferred β crystal orientation after hydrogen-induced recrystallization.

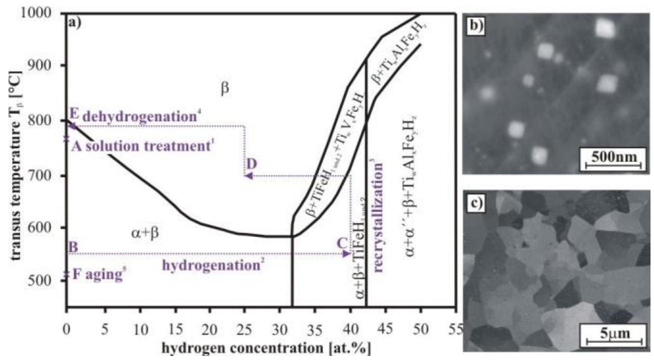

Figure 8. (a) HIRB-THT strategy inscribed schematically by ABCDEF in the T_β diagram; FE-SEM micrographs after THT-steps (b) hydrogenation (BC) and (c) recrystallization (CD).

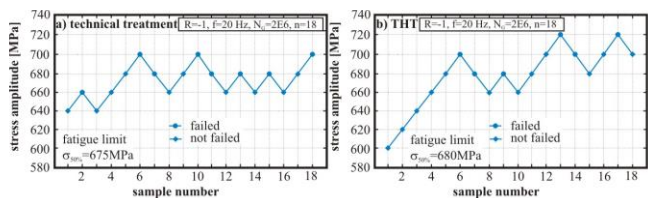

Figure 9. Results of the staircase test applied to (a) conventional technical heat treatment as reference condition and (b) 5-step HIRB-THT treated material (sequence of tests).

Fatigue crack initiation at the sample surface indicated a microstructural homogeneity after the HIRB-THT process. The fatigue crack propagation measurements of single edge notch bend (SENB) samples were carried out under cyclic 4-point bending loading according to ASTM-E647. The determination of long crack growth behavior at a stress ratio of R = 0.1 according to the load shedding method indicated that the fatigue crack growth threshold ΔK_{th} in the peak-aged HIRB-THT condition is below 2.0 $MPam^{0.5}$. The crack propagation resistance of the technical heat treated condition is 2.3-3.5 $MPam^{0.5}$. As expected, the hydride-induced precipitation hardening of the β matrix of the HIRB-THT condition causes no improvement of the long crack growth behavior, which is generally deteriorated by the precipitation hardening of the β matrix. This is characteristic for precipitation-hardenable metastable β titanium alloys.

Fundamental Research

Microstructural Dependence of HCF in Ti 6Al 2Sn 4Zr 6Mo

The microstructural dependence of high cycle fatigue (HCF) and multi-competing crack nucleation in Ti 6Al 2Sn 4Zr 6Mo alloy has been studied at the TU Clausthal. The comparison of HCF performance of various microstructures of Ti 6Al 2Sn 4Zr 6Mo was conducted via rotary bending fatigue tests. D10 (homogenization: 990°C/1h/WQ, rolling at 900°C, degree of deformation 1.4, recrystallisation: 920°C/1h/AC, ageing: 595°C/8h/AC) exhibits the optimal fatigue strength, succeeded by β annealed (990°C°C1h/AC) and D30 (900°C/1h/AC). Pronouncedly enhanced fatigue lifetimes were achieved in D10 compared to the as received condition in particular, as shown in Figure 10. The outperformance of D10 compared to β annealed is supposed to be attributed to the occurrence of very fine particle-like secondary alpha (α_s) in duplex structures instead of lamellae-shaped α_s in other (α + β) alloys such as Ti 6Al 4V, which leads to decreased slip length and thus less or even none negative influence from α colony size effect in the duplex structures [17]. Isothermal fatigue tests on D10 at both room and 450℃ showed that the increase of test temperature results in little deterioration in HCF of D10, referred to the as received reference (see Figure 11).

A fractographic study using SEM reveals cracks in D10 nucleating at surface or subsurface, and even dual subsurface initiated cracks occurred, as shown in figure 12a. This confirms the proposition of J.M. Larsen [18] that different microstructural configurations may compete with each other to initiate the dominant fatigue crack. Multi-crack nucleation modes were observed, such as synergistic faceting through a group of αp or step-wise faceting. A fractograph of the latter is displayed in figure 12b. EDX exhibits similar chemical composition of the

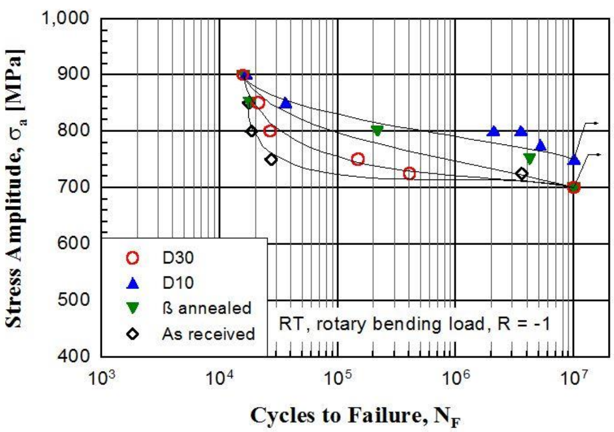

Figure 10. Comparison of fatigue behaviour of D30, D10, β annealed and as received condition,

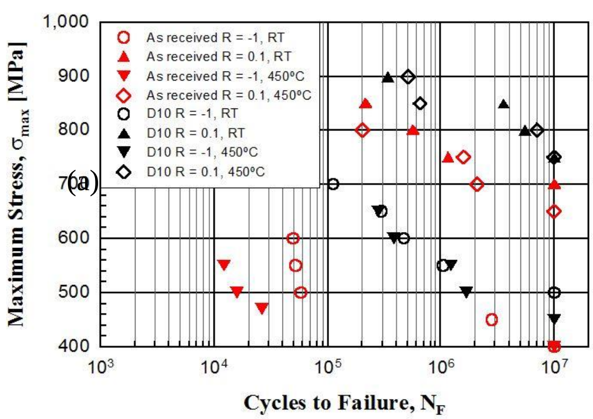

Figure 11. Isothermal fatigue behaviour of D10 at both load ratio R = -1 and 0.1 compared to as received.

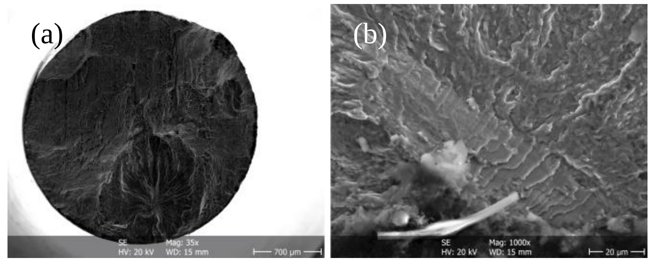

Figure 12. (a) Dual subsurface crack nucleation, (b) step-wise faceting.

facet to that of α_p. A. Pilchak [19] concluded similar fracture features in Ti 6Al 4V as the result of low angle faceting parallel to the basal plane in α grains.

ω-phase Precipitation in Ti 15Mo Alloy

The titanium alloy Ti 15Mo is a metastable β alloy of the second generation for medical applications. This alloy does not contain known toxic elements like aluminium or vanadium. In the solution treated state the Young's modulus is comparatively low. Therefore, the stress-shielding effect is diminished by this but the static strength is relatively low too, so an increase in strength by precipitation hardening is required for implants of Ti 15Mo.

To increase the strength, the precipitation of ω-phase in Ti 15Mo was investigated after heat treatments at temperatures between 225°C and 350°C for 5 minutes up to 240 hours. The phase composition was studied by hard X-ray analyses and the resulting mechanical properties of Ti 15Mo alloy have been investigated. In addition the ω-formation, ω-growth and its transformation to α-phase has been studied. First, nano-sized, round ω-precipitations develop homogenously which grow in preferred orientations and finally transform to plate-like α-phase (above 400°C).

In general, the ω-phase caused an increase in strength and the Young's modulus of the alloy whereas the ductility strongly decreased (see Figure 13). Nevertheless, low amounts of nano-crystalline ω-phase can lead to an improved fatigue limit by about

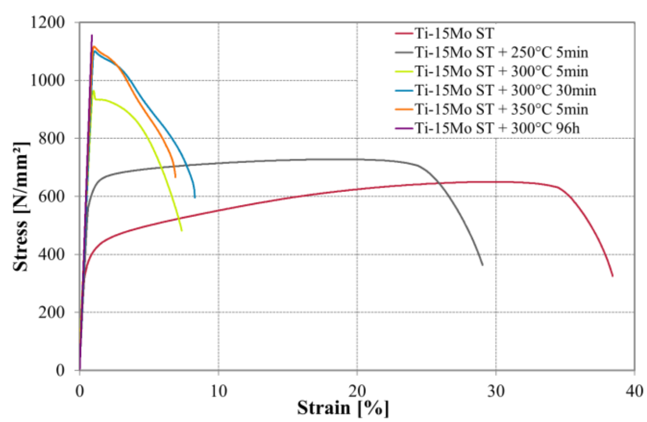

Figure 13. Stress-strain curves of Ti 15Mo in different ageing states. ST: solution treated at 800°C/0.5h/WQ. With increasing ageing temperature the stress is increasing while the ductility is decreasing.

60% compared to the solution treated state. The results show that strengthening of metastable β-alloys by ω-phase distribution is feasible [20, 21].

Analyses of Titanium's Oxidation Behaviour

Due to their relatively poor oxidation resistance, conventional titanium alloys can only be applied up to approx. 550°C. It is known that the addition of niobium decelerates the oxidation of titanium alloys whereas elements like vanadium do not improve titanium's oxidation resistance. The underlying mechanisms are not yet well understood. In the present research cooperation between the TU Braunschweig and the University of Edinburgh different binary titanium-niobium and titanium-vanadium alloys as well as commercially pure titanium were investigated. Oxidation experiments were carried out at 800°C up to 288 hours followed by metallographic analyses to study the oxide layer morphology as well as the microstructure at the interface. Energy-dispersive X-ray spectroscopy mappings were used to identify possible changes in the distribution of the alloying elements. In addition, micro-focused hard X-ray experiments were performed to layer-wise analyse the phase composition (see Figure 14).

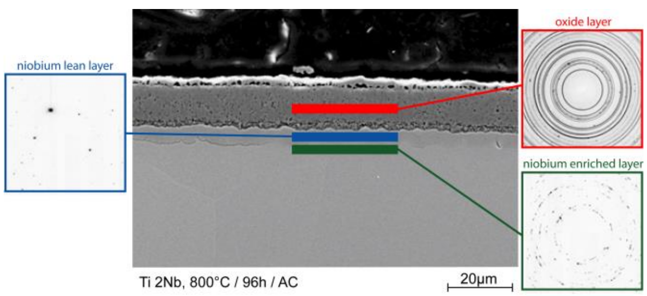

Figure 14. Micro-focussed hard X-ray analyses at Ti 2Nb after 96 hours of oxidation at 800°C performed at beamline P07 of PETRA III, DESY. The bars in the figure represent the exposure volume. A three-layer structure composed of the oxide (red), a niobium lean layer (blue) and a niobium enriched layer (green) has been overserved.

As expected, the niobium containing alloys show a better oxidation performance compared to commercially pure titanium and the titanium-vanadium alloys. The oxide layer consisted of TiO_2 and Ti_2O_3. Depending of the niobium content, a niobium enriched layer developed below the metal-oxide-interface minimising oxygen diffusion into the titanium matrix. In case of vanadium no vanadium enriched layer was found. The experimentally obtained results are in good agreement with density functional theory simulations.

Based on these results, the minimal niobium content needed for improved oxidation resistance was identified so that alloys of technical relevance can now be developed [22].

Shear Melting during Segmented Chip Formation of Titanium

In machining, three different kinds of chips are known to form: continuous chips, segmented chips, and completely separated segments. The chip formation process during metal machining can be described as follows: In the beginning of the cutting action, the tool penetrates the workpiece and the material is dammed in front of the tool. The plastic deformation is concentrated in a narrow zone, the so-called primary shear zone leading from the tool tip to the upper surface of the workpiece. Most of the energy used for the plastic deformation is transformed into heat in this primary shear zone. If the heat can dissipate quickly into the areas surrounding the primary shear zone, the material is deformed homogeneously leading to the formation of a continuous chip with constant thickness and the cutting force remains almost constant. On the other hand, if the heat cannot dissipate quickly into the material surrounding the primary shear zone, heat is concentrated there, the material may locally soften and the deformation may become localised. In this case, deformation only occurs in a narrow zone of a few microns (the so-called adiabatic shear band) which leads to the formation of segmented chips [22].

It is known that mainly α-titanium containing alloys like CP-Titanium or Ti 6Al 4V form segmented chips under almost any cutting condition even at very low cutting speeds and cutting depths. In contrast, solution treated metastable β-titanium alloys like Ti 15V 3Al 3Sn 3Cr undergo a cutting-speed dependent change in their chip-formation process from continuous (at low cutting speeds) to segmented (at high cutting speeds) chips. Segmented chips are more commonly obtained from aged metastable β-alloys.

There are many atomic-level mechanisms for deformation in metals, dislocation motion is the easiest and slowest, while high shear rate can give rise to twinning, and grain boundary sliding is important in nanocrystalline materials. Titanium alloys are notable for their very poor heat conduction, which means that temperature within a shear band may rise towards the melting point as the energy from the deformation remains localised. Shear localisation implies very high shear rates within the band (strain rate $> 10^7\ s^{-1}$): the overall shear rate is increased locally by the degree of localisation [23].

In the current study (see Figure 15), molecular dynamics simulations of shear at high rates and various temperatures have been run. A dynamic transition in the mode of shear deformation was observed. Up to 900K, the deformation proceeds by dislocation motion which changes the shape of each grain. Some coarsening of the microstructure can also be seen. Above 1400K, the mechanism is similar, until about 50% strain, at which point a two phase structure appears spanning the system. Even with a few million atoms, all the shear is concentrated in the localised non-crystalline region. We describe this region as amorphous,

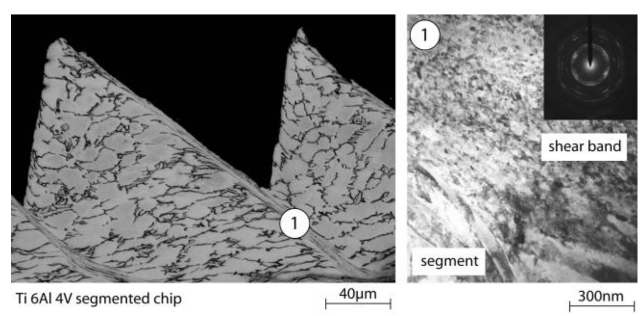

Figure 15. During machining of Ti 6Al 4V alloy segmented chips develop. The individual segments are separated by a shear band (left). The shear band consists of a nano-crystalline microstructure (right).

while recognising that at these short lengths and timescales the distinction between this and a liquid is arbitrary. Within the amorphous region, small nanocrystallites survive and move in a correlated manner within disordered liquid-like surroundings. The central result is that the shear becomes localised in an amorphous region which has almost liquid-like properties. These results are in good agreement with experimental investigations (see Figure 15) [24, 25].

Electrodeposition of Titanium Alloys from Molten Salt

The electrodeposition of titanium alloys form molten salts is investigated in collaboration between the Institute of Process Metallurgy and Metal Recycling (RWTH Aachen) and the Institute of Materials Research (German Aerospace Center). Such processes can be used for the production of monofilament reinforced titanium matrix composites [26]. The applicability has been demonstrated for titanium [27]. However, the full potential of titanium matrix composites cannot be exploited with a pure titanium matrix.

A current project deals with the synthesis of the alloy Ti 6Al 4V. For this purpose first the binary systems Ti-V and Ti-Al are studied, which is the basis for the ternary system Ti-Al-V. The main idea is to dissolve the elements individually from anodes of the corresponding metals and deposit them simultaneously on the cathode. This requires a systematic investigation of the anodic and cathodic subprocesses of all elements individually and in combination.

The experiments are carried out in a glovebox system with high purity argon atmosphere. Exemplarily for the cathodic subprocess, Figure 16 shows details of a typical experiment: In a first step LiCl-KCl-$TiCl_2$ (green) and LiCl-KCl-VCl_3 (purple) are molten individually. Subsequently, pieces of the solidified salts are remolten together in one crucible. After melting, the Ti and V ions mix in the electrolyte, and during electrolysis the ions of both elements are co-deposited on the cathode. EDS measurements (see Figure 17a) on a cross section of a coated tungsten cathode indicate a quite constant vanadium content within the titanium deposit (see Figure 17b).

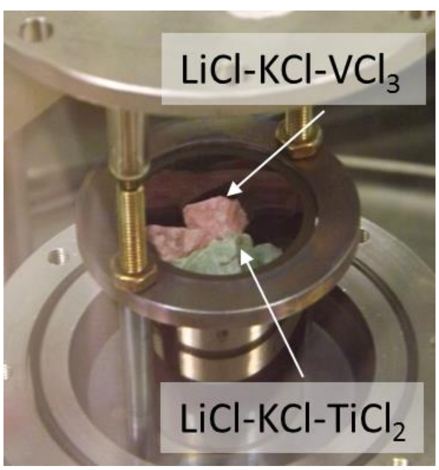

Figure 16. Detail of experimental setup. Glassy carbon crucible with solidified pieces of LiCl-KCl-$TiCl_2$ (green) and LiCl-KCl-VCl_3 (purple).

The investigation of the anodic subprocess revealed, that Al and V anodes dissolve in the base electrolyte LiCl-KCl without difficulty. However, passivation phenomena were observed in LiCl-KCl-$TiCl_2$, which may be explained by the high reactivity of the titanium ions. The exact mechanisms of these reactions are subject to further investigation.

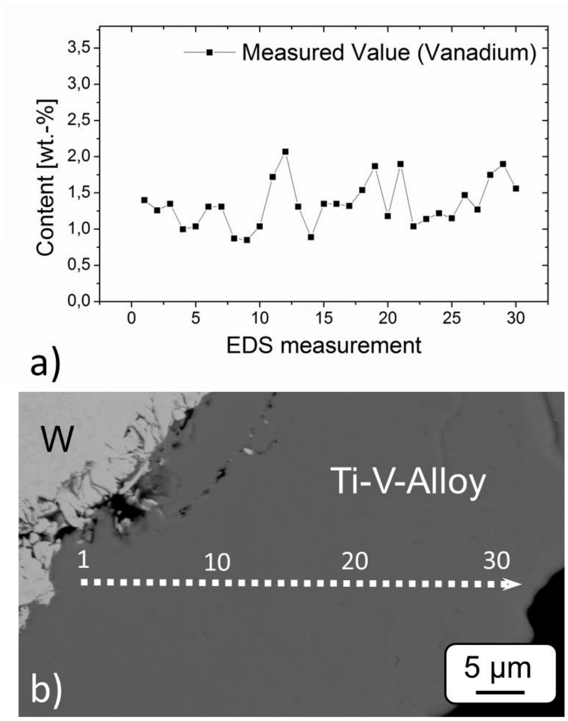

Figure 17. (a) Results of EDS line scan carried out on cross section of Ti-V-alloy electrodeposited (b) on a tungsten wire.

Thermomechanical Fatigue Behaviour of Titanium Aluminides

In recent times, γ-TiAl-based alloys have found large-scale implementation as blade material into advanced aero engines, substituting heavy-weight nickel-based alloys. However, a remaining crucial issue is to assess the material's maximum reliable fatigue and to develop a suitable fatigue life prediction model for both low cycle fatigue (LCF) and thermomechanical fatigue (TMF) conditions.

Investigations conducted at the Universität Siegen have revealed that the high-temperature low cycle fatigue behaviour of the advanced γ-TiAl-based alloy Ti 45Al 8Nb 0.2C (TNB-V2), containing 8 at.-% niobium, is rather modest at an applied total strain amplitude of $\Delta\varepsilon/2 = 0.7\%$ under fully-reversed testing conditions. In the temperature field between room temperature and 850°C, fatigue life never exceeded 600 cycles.

Recent results on the LCF and TMF behaviour of TNB-V2 at lower strain amplitudes show a significant increase in the fatigue life. The different fatigue performance can be correlated with the amount of plastic strain amplitude. The amount of plastic strain amplitude almost doubles between total strain amplitudes from 0.6 to 0.7%. In this study a model was developed to predict the fatigue life of γ-TiAl-based alloy TNB-V2 under LCF and TMF conditions. In the first part of this model the TMF hysteresis loop was simulated by means of a multi-component model using only the LCF data. In order to simulate the hysteresis loops for the complete test microstructure changes as well as hardening and softening processes were integrated. Figure 18 shows a comparison between a simulated and obtained TMF hysteresis loop at the beginning of the test as well as at the half of the fatigue life ($N_f/2$).

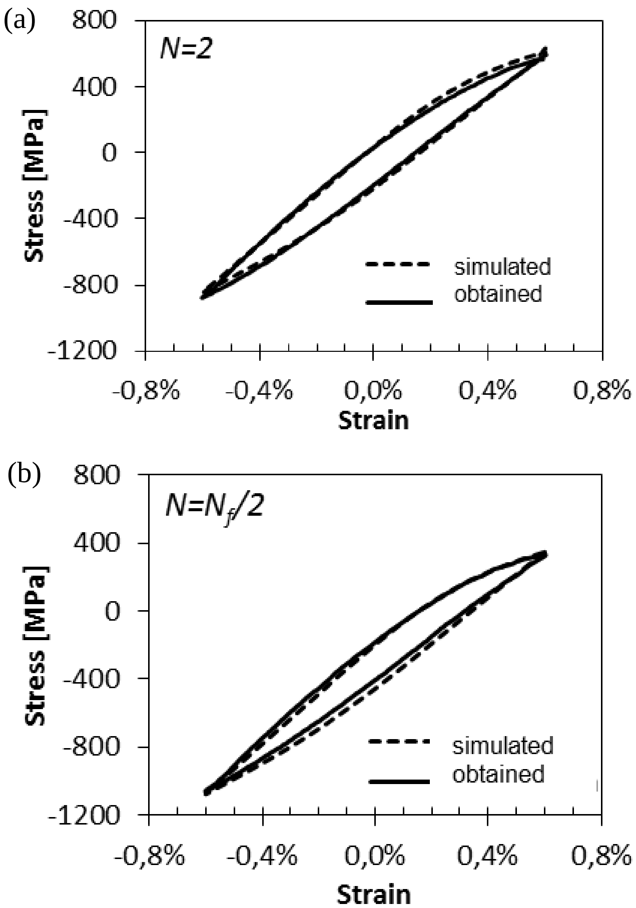

Figure 18. Suitable agreement between simulated and obtained TMF hysteresis loop at the beginning (a) of the test as well as at the half (b) of the fatigue life (Nf/2).

In the second part of the model a damage parameter was defined, which includes the temperature as a physical dimension and takes into account the effect of the mean stresses

$$P_{Ges} = \frac{p_{max} + p_{min}}{2} + p_m^{\alpha_{R_p}} = \frac{1}{2}\left(\frac{\sigma_{ZUP}}{R_{p0,2}(T_{\sigma_{ZUP}})} + \frac{\sigma_{DUP}}{R_{p0,2}(T_{\sigma_{DUP}})}\right) + p_m^{\alpha_{R_p}}$$

in which p_{max}, p_{min} and p_m are the damage factors caused by tension stress, compression stress and mean stress, respectively, σ_{ZUP} and σ_{DUP} are the stress at the tensile reversal point and compression reversal point, respectively, α_{Rp} is a material depending coefficient.

The parameters in terms of upper and lower stresses needed for this model were calculated by means of the multi-component model mentioned above. The results of the fatigue life prediction model under LCF and TMF conditions are shown in Figure 19.

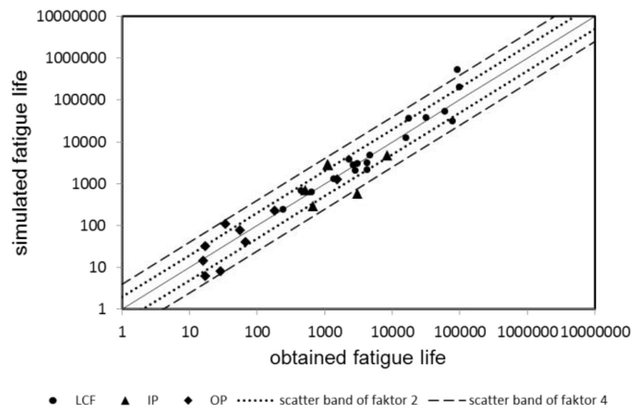

Figure 19. Comparison between the obtained and the calculated fatigue life under TMF and LCF conditions.

Acknowledgements

Contributions to this plenary paper from different industrial companies, research organisations and universities are gratefully acknowledged: Colleagues from VDM Metals GmbH (J. Kiese), GfE Metalle und Materialien GmbH (M. Achtermann, H. Keitel), MTU Aero Engines (U. Habel), Litos/ (D. Wolter), the Fraunhofer IFAM (M. Jurisch), the German Aerospace Center (J. Gussone, J. Haubrich), the RWTH Aachen (K. Milicevic, B. Friedrich), the Technische Universität Braunschweig (F. Brunke), the Technische Universität Clausthal (L. Wagner, M. Wollmann, S. Yang), University of Edinburgh (G. Ackland), the Montan Universität Leoben (H. Clemens) and the Universität Siegen (H.-J. Christ, A. El-Chaikh, V. Macin, P. Schmidt,) added their results to highlight the titanium research activities of the least four years.

References

1. R.A. Yokel, D.D.Allen, and D.C. Ackley, “The distribution of aluminium into and out of the brain”, *Journal of Inorganic Biochemistry*, 76 (1999), 127-133.

2. C. Siemers, D. Wolter, and H. Sibum, „Hochfester Titanwerkstoff auf Basis technisch reinen Titans (CP-Titan)“, German Patent Application Nr. 10 2014 010 032.4, submitted in July 2014.

3. W. Smarsly, S. Mayer, and H. Clemens, “Advanced Intermetallic Titanium Aluminides - Development Status and Perspectives“ (Paper presented at the Intermetallics 2013, Banz, Germany, 30 September 2013).

4. W. Smarsly, and D. Gopal “Development of gamma TiAl for gas turbine engines” (Paper presented at the International Workshop on Gamma Alloy Technology, Toulouse, France, 11 June 2013).

5. W. Smarsly, “Triebwerkswerkstoffe, Quo vadis” (Paper presented at the 60. Metallkunde-Jubiläumskolloquium Montanuniversität Leoben, Lech am Arlberg, Austria, 23 April 2014).

6. H. Wang, Z. Z. Fang, P. Sun, “A critical review of mechanical properties of powder metallurgy titanium”, *International Journal of Powder Metallurgy*, 16 (5) (2010) 45-57.

7. M. Jurisch, et al., “3D screen printing for the fabrication of small intricate Ti-6Al-4V parts” (Paper presented at the Euro PM2014, Salzburg, Austria, 21 September 2014).

8. C.A. Stubbington, and A.W. Bowen, “Improvements in the fatigue strength of Ti-6Al-4V through microstructure control”, *Journal of Materials Science*, 9 (1974) 941-947.

9. T. Ebel, et al., “Metal injection moulding of titanium and titanium-alluminides”, *Key Engineering Materials*, 520 (2012), 153-160.

10. T. Ebel, “Advances in the Metal Incection Mouldong of Titanium at Euro PM2014”, *PIM International*, 9 (1) (2015), 51-61.

11. Y.F. Yang et al., “Impurity scavenging, microstructural refinement and mechanical properties of powder metallurgy titanium and titanium alloys by a small addition of cerium silicide”, *Materials Science and Engineering A*, 573 (2013), 166-174.

12. R.M. German, “Progress in Titanium Metal Powder Injection Moulding”, *Materials*, 6 (2013), 3641-3662.

13. P. Schmidt, A. El-Chaik, and H.-J. Christ, “Effect of duplex aging on the Initiation and propagation of fatigue cracks in the solute-rich metastable β titanium alloy Ti 38-644”, *Metallurgical and Materials Transaction* A, 42(9) (2011), 2652-2667.

14. P. Schmidt, V. Macin, and H.-J. Christ, “Thermohydrogen treatment of highly beta-stabilized titanium alloy Ti 38-644 (Beta-CTM)” In: B.P. Somerday, and P. Sofronis (Eds.), *Hydrogen-materials interactions* (New York, USA: ASME, 2014), 661-668.

15. V. Macin, and H.-J. Christ, “Hydride-induced microstructure optimization of high-strength beta titanium alloy Ti 10-2-3 by thermohydrogen treatment” (Paper presented at the LightMat 2013, Bremen, Germany, 3 September 2013), 1-6.

16. V. Macin, P. Schmidt, and H.-J. Christ, “Thermohydrogen treatment of high strength beta titanium alloy Ti 10V-2Fe-3Al”. In: B.P. Somerday, and P. Sofronis (Eds.). *Hydrogen-materials interactions*. (New York, USA, ASME, 2014), 669-676.

17. G. Lütjering, “Property optimization through microstructural control in titanium and aluminum alloys”, *Materials Science and Engineering A*, 263 (1999), 117-126.

18. J.M. Larsen, C.J. Szczepanski, and S.K. Jha, “The role of microtexture on the fatigue behaviour of an $\alpha + \beta$ Titanium alloy, Ti-6Al-2Sn-4Zr-6Mo”, in *VHCF4*, J. Allison et al. (Eds.), TMS, Warrendale, PA, 2007, 385-396.

19. A. Pilchak, et al., “Low ΔK faceted crack growth in titanium alloys”, *International Journal of Fatigue*, 31 (2009), 989-994.

20. F. Brunke, L. Waalkes, and C. Siemers, “Deformability of the rare earth metal modified metastable-β alloy Ti-15Mo”, *International Journal of Chemical, Nuclear, Metallurgical and Materials Engineering*, 8 (11) (2014), 1073-1077.

21. F. Brunke, N. Holzapfel, and C. Siemers, “Optimisation of Machining Processes of the Metastable-β Alloy Ti-15Mo for Implant Applications” (Paper presented at the the LightMAT 2013 Conference, Bremen, Germany, 3 September 2013).

22. C. Siemers, et al., “Development of Oxidation Resistant Titanium Alloys by Niobium Addition” (Paper presented at the COM2014, Vancouver, Canada, 28 September 2014).

23. J. Rösler, M. Bäker, and C. Siemers, “Mechanisms of Chip Formation”, in: H.K. Tönshoff und F. Hollmann: *Hochgeschwindigkeitsspanen metallischer Werkstoffe* (Weinheim, Germany: Wiley-VCH, 2005), 492 – 515,

24. K. Saksl, et al., “Local structure of metallic chips examined by X-ray microdiffraction”, *Journal of Alloys and Compounds*, 581 (2013), 579 – 584.

25. C. Healy, et al. “Shear melting and high temperature embrittlement: Theory and application to machining titanium”, *Physical Review Letters*, (2015), in print.

26. C. Leyens, J. Hausmann,, and J. Kumpfert, “Continuous Fiber Reinforced Titanium Matrix Composites: Fabrication, Properties, and Applications”, *Advanced Engineering Materials*, 5 (6) (2003), 399-410.

27. J. Gussone, and J. Hausmann, “Deposition of titanium on SiC fibres from chloride melts”, *Journal of Applied Electrochemistry*, 41(6) (2012), 657-662.